

Plasma beam structure diagnostics in krypton Hall thruster

Agnieszka Szelecka¹, Maciej Jakubczak^{1,2} and Jacek Kurzyna¹¹Institute of Plasma Physics and Laser Microfusion, Hery 23 01-497 Warsaw, Poland and ²Faculty of Physics, Warsaw University of Technology, Koszykowa 75 00-662 Warsaw, Poland

Research Article

Cite this article: Szelecka A, Jakubczak M, Kurzyna J (2018). Plasma beam structure diagnostics in krypton Hall thruster. *Laser and Particle Beams* **36**, 219–225. <https://doi.org/10.1017/S0263034618000198>

Received: 15 December 2017

Accepted: 22 February 2018

Key words:

Beam divergence; Faraday probe; krypton Hall thruster; Langmuir probe; plasma diagnostics

Author for correspondence:Agnieszka Szelecka, Institute of Plasma Physics and Laser Microfusion, Hery 23 01-497 Warsaw, Poland, E-mail: agnieszka.szelecka@ifpilm.pl**Abstract**

Krypton Large Impulse Thruster (KLIMT) project was aimed at incremental development and optimization of a 0.5 kW-class plasma Hall Effect Thruster in which, as a propellant, krypton could be used. The final thermally stable version of the thruster (the third one) was tested in the Plasma Propulsion Satellites (PlaNS) laboratory in the Institute of Plasma Physics and Laser Microfusion (IPPLM) in Warsaw as well as in the European Space Agency (ESA) propulsion laboratory in the European Space Research and Technology Centre (ESTEC).

During final measurement campaign, a wide spectrum of parameters was tested. The plasma potential, electron temperature, electron concentration, and electron energy probability function in the far-field plume of the thruster were measured with a single cylindrical Langmuir probe. Faraday probes were used for recording local values of ion current. Using several collectors in different locations and moving them on the surface of a sphere, the angular distribution of the expelled particles was reconstructed which was a local measure of beam divergence. Angular distribution of ion flux as measured with a central Faraday probe was parameterized with krypton mass flow rate, voltage, coil current ratio, and the cathode mass flow rate. Beam divergence measurements with Faraday probes as well as plasma parameters derived from Langmuir probe seem to be consistent with our understanding of the operating envelope. Obtained results will serve as a baseline in the design of plasma beam structure diagnostics system for the PlaNS laboratory.

Introduction

Hall thruster, also called Hall Effect Thruster (HET) or Stationary Plasma Thruster, is a type of electric propulsion device that was invented more than 50 years ago in Soviet Union (Zhurin *et al.*, 1999). This type of thruster is considered for many space applications ranging from the positioning of nearby satellites to being the main propulsion in deep-space missions, and since its first use on Meteor satellite in 1971 (Morozov, 2003), there was a growing interest in this technology that resulted in several space-qualified and many laboratory models of different geometries and types of propellant.

Hall thruster, in its basic configuration (Goebel and Katz, 2008; Boeuf, 2017), is a cylindrical device with an anode (acting simultaneously as a gas distributor) inside a ring-shaped insulating channel, an external cathode outside and a magnetic circuit, as seen in Figure 1. Between the anode and cathode, a constant voltage is applied that creates axial electric field, whereas two magnetic coils form strong radial magnetic field inside the channel. These perpendicular fields trap part of electrons emitted from the cathode, causing them to drift azimuthally in the direction at the end of the thruster channel. High electron density in this region causes efficient ionization of the gas particles coming out of the anode and low electron mobility in the axial direction form a steep electric potential drop on which the newly formed ions are rapidly accelerated and ejected from the device, thus generating thrust. The remaining electrons from the cathode act to neutralize these ions.

Within the frames of the European Space Agency (ESA)/Plan for European Cooperating States (PECS) program in the Plasma Propulsion Satellites (PlaNS) laboratory, the Krypton Large Impulse Thruster (KLIMT) project, a 0.5 kW-class HET, was developed (Kurzyna *et al.*, 2014, 2016; Szelecka *et al.*, 2017). It was designed to work with krypton propellant as a cost-effective alternative to xenon that is commonly used in these thrusters.

The main thruster parameters, such as thrust, efficiency, and specific impulse, depend strongly on the structure and divergence of the emitted plasma beam. Thus, to fully understand the measured thrust values for different operating regimes of the thruster, it is necessary to have beam diagnostics of the far-field plasma plume. KLIMT was tested in terms of thrust in both PlaNS and ESA electric propulsion laboratories, but only in the latter beam diagnostics (Faraday probes) were also available.

In this work, the beam shape and divergence measurements from Faraday probes in the ESA EP laboratory are presented. Additionally, shown are preliminary values of plasma

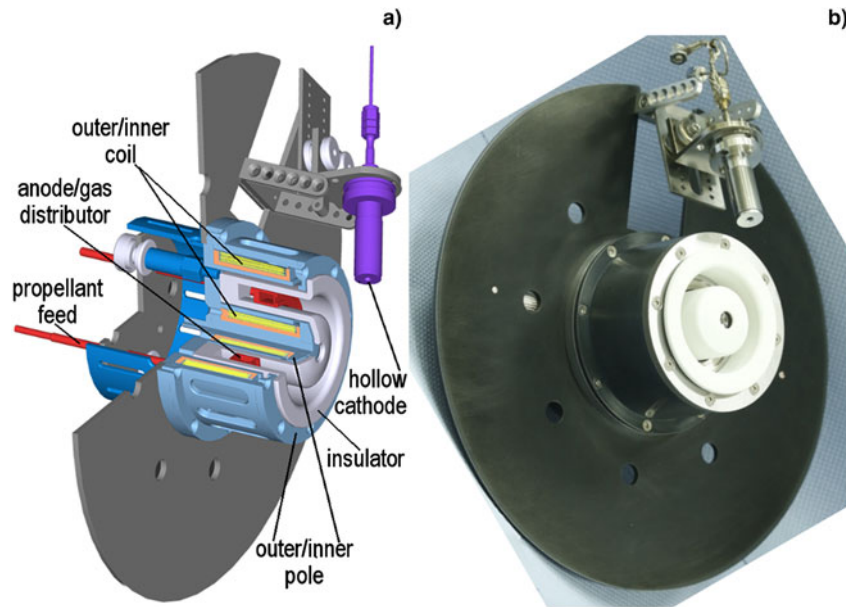


Fig. 1. KLIMT third prototype – cross-section (left) and photograph (right).

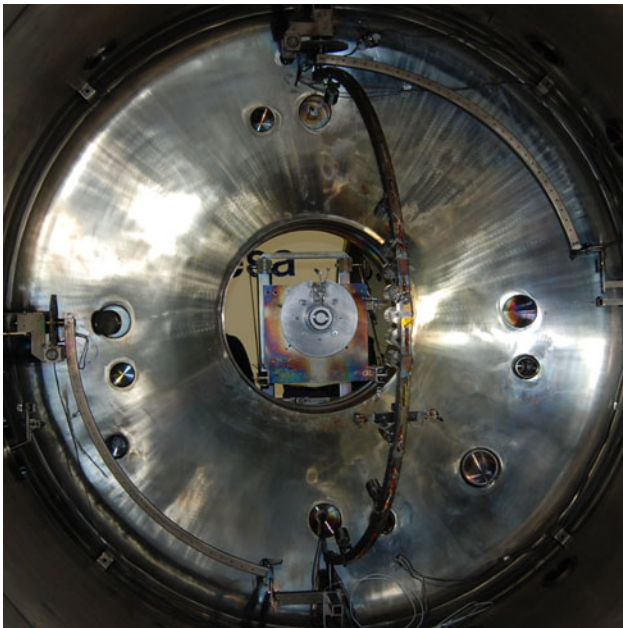


Fig. 2. Faraday probes in ESTEC laboratory.

parameters obtained from Langmuir Probe diagnostics manufactured in PlANS. The results as well as understanding of possibilities and limitation of both methods will serve as a baseline in the design of beam diagnostics system for the PlANS laboratory in the IPPLM.

Faraday probes

The Faraday probes were used to determine the ion current density distribution in the far-field plume of the thruster. Exactly 11 collimated Faraday probes were mounted on a semi-circular arm rotating around a vertical axis. The arm was connected via a gearbox to a stepper motor that allowed a full 180° rotation. The

Faraday probes covered the entire beam from the thruster. The external diameter of the arm and its width were, respectively, 75 and 3 cm. The distance between the thruster exit plane and the arm center of rotation was measured and taken into account during the post-processing of the data collected by the Faraday probes. The collected current was measured with a current probe. The current value and the collection area of the probe gave the current density at the location of the probe. This measurement was corrected in order to take into account the distance between the center of the arm and the thruster exit plane. The collimated FPs were equipped with a collimator placed in front of the probe (78.5 mm²) and a molybdenum collector used to minimize secondary electron emission and sputtering phenomena due to erosion. The collector was biased negatively with respect to the plasma potential to repel primary electrons. To eliminate disturbances, a stainless steel external shield was used, and to ensure electric insulation, a teflon body was used.

The picture in Figure 2 presents a view from front of the open vacuum chamber in ESTEC laboratory. In the foreground, we can see the Faraday probes on the rotating arm and in the background the KLIMT thruster fixed to the hatch.

Jet momentum losses due to beam divergence are expressed as a momentum-weighted average quantity from the formulation of thrust what is equal to the ratio of the measured thrust component directed along the thruster centerline relative to the theoretical thrust achieved when all ions are traveling parallel to the thruster centerline. Momentum losses associated with plume divergence may be calculated with knowledge of the total mass flow rate, measured thrust, and the mass-weighted average velocity. The momentum-weighted average divergence can be also approximated as the charge-weighted average divergence for an axisymmetric plume.

$$\cos\theta_j^2 = \left(\frac{2\pi R^2 \int^j(\theta)\cos(\theta)\sin(\theta)d\theta}{2\pi R^2 \int^j(\theta)\sin(\theta)d\theta} \right)^2.$$

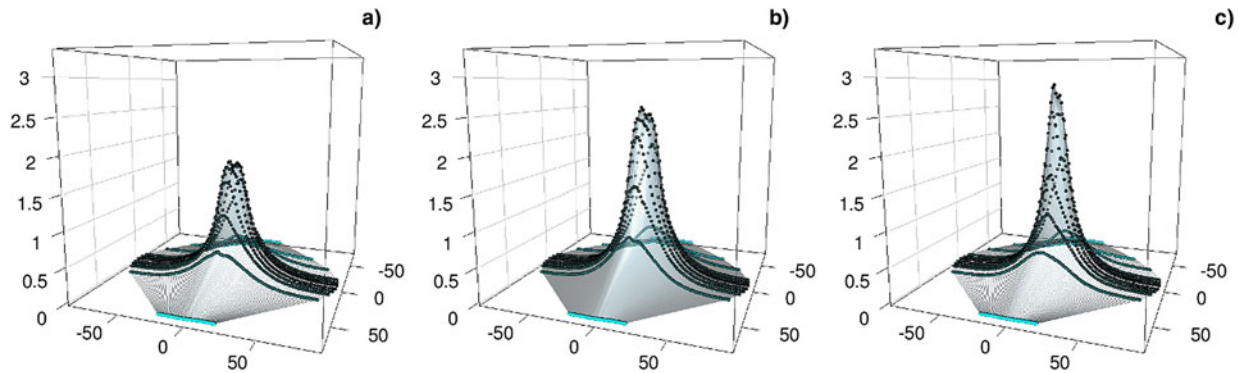


Fig. 3. The 3D profiles of ion charge flux for different operating conditions: (a) $U_d = 240$ V, $I_{inn} = 5.0$ A, $I_{out} = 2.5$ A, $m_c = 1$ sccm, $m_a = 1$ mg/s; (b) $U_d = 260$ V, $I_{inn} = 5.0$ A, $I_{out} = 2.0$ A, $m_c = 1$ sccm, $m_a = 1.19$ mg/s; (c) $U_d = 300$ V, $I_{inn} = 5.0$ A, $I_{out} = 2.0$ A, $m_c = 3$ sccm, $m_a = 1$ mg/s.

Off-axis cosine losses integrated in the numerator of above equation quantify the axial component of beam current that generates thrust. Beam efficiency is evaluated as a charge-weighted average cosine, which is equal to the square of the axial component of ion beam current relative to the total ion beam current as measured by a Faraday probe (Brown, 2009).

In order to characterize the beam, 3D and 2D profiles of ion charge flux were created. In Figure 3 are shown three profiles with the thruster working in different operating conditions. The 2D profiles from the main (central) Faraday probe with respect to the discharge voltage, magnetic field topography (controlled by coil currents), and mass flow rates from anode and cathode, as well as the corresponding angles of divergence are presented in Figure 4. The summary plots for all investigated cases are in Figure 5.

The obtained results demonstrate that shape of the profile depends on all the controlled variables – applied voltage, magnetic field strength, and topography (controlled by coil currents) and gas mass flow rates. It was observed that beam divergence strongly decreases as the voltage applied increases for all cases. This is due to the fact that higher discharge voltage corresponds to higher axial electric field, thus larger axial velocities of the accelerated ions. Bigger ratio of axial to transverse ion velocities results in smaller divergence of the beam. It was noted that the magnetic field also strongly influences the shape of this beam, as it should. For the case presented, it seems that for the same field shape (coil currents ratio) smaller field magnitude lowers the beam divergence, although the amount of data is insufficient to draw any conclusions as to the general tendency. In addition, it was noted that the increased gas flow through the anode causes the beam to slowly expand, but also that the gas flow through the cathode causes minor differences in its appearance.

Langmuir probe

Langmuir probe is a small electrode, typically cylindrical, spherical, or planar in shape, inserted into plasma and polarized in wide range. Only the ions and electrons with energies sufficient to cross plasma sheath of the probe are collected and so current–voltage characteristics can be obtained (Fig. 6). Then, from the current–voltage (I – V) curves of the probe, several plasma parameters can be calculated.

To measure some of the plasma parameters in the far-field plume of the Hall thruster, a single cylindrical Langmuir probe

was manufactured in the IPPLM PlaNS laboratory (Fig. 7) together with a dedicated power supply unit. The electrode of the probe was made from 0.2 mm-thick tungsten wire with the collecting part 9.2 mm long. The probe was positioned in the thruster axis at a distance of approximately 470 mm from the channel exit and was aligned with the plasma flow, so the current to the probe resulted mainly from the thermal motion of the electrons and ions. The probe current–voltage characteristics were collected in the range of -60 to 30 V with the measured current signal averaged over 256 traces on an oscilloscope for each point.

Several different processing routines that provide for electron current separation (Steinbruchel, 1990; Chen *et al.*, 2002; 2003; Raites *et al.*, 2005; Merlino, 2007; Godyak and Alexandrovich, 2015), electron energy probability function reconstruction (Druyvesteyn, 1930; Godyak and Demidov, 2011; Godyak and Alexandrovich, 2015), and plasma parameter calculation (Steinbruchel, 1990; Chen *et al.*, 2002; 2003; Conde, 2011; Godyak and Demidov, 2011; Godyak and Alexandrovich, 2015) were examined. Using various methods of electron current separation, it was decided that a simple linear fit of ion current I_i gave the best agreement with the experimental results and this method was used throughout the analysis. Plasma (space) potential was obtained as the point on I – V curve where a knee in exponential growth of electron current I_e occurs [i.e., where $I_e'(V) = \max$]. Electron energy probability function was calculated with the Druyvesteyn method that uses the second derivative of the electron current, which was computed using approximating spline functions to avoid numerical noise. Because it was found that in our case I_i was approximately linear with V , then $I_i'' = 0$ and $I_e'' = I''$. It was noted that the assumption about Maxwellian electron energy probability function ($f_M(\epsilon) \sim \sqrt{\epsilon} \exp(-\epsilon/a)$) that is made for most of the methods was not satisfied in our conditions, as seen in Figure 8. The obtained electron energy probability function resembles the so-called Druyvesteyn distribution ($f_D(\epsilon) \sim \sqrt{\epsilon} \exp(-\epsilon^2/b)$) that is reported to be related to the dominance of elastic collisions between electrons and neutrals in plasma, in which the energy transfer is not effective and electrons cannot thermalize (Godyak and Demidov, 2011). Therefore, electron concentration and temperature were derived directly from the electron energy probability function (Godyak and Demidov, 2011; Godyak and Alexandrovich, 2015) and not the classical Langmuir analysis.

The resulted space potential V_s , electron temperature T_e , and electron concentration n_e for some typical working conditions

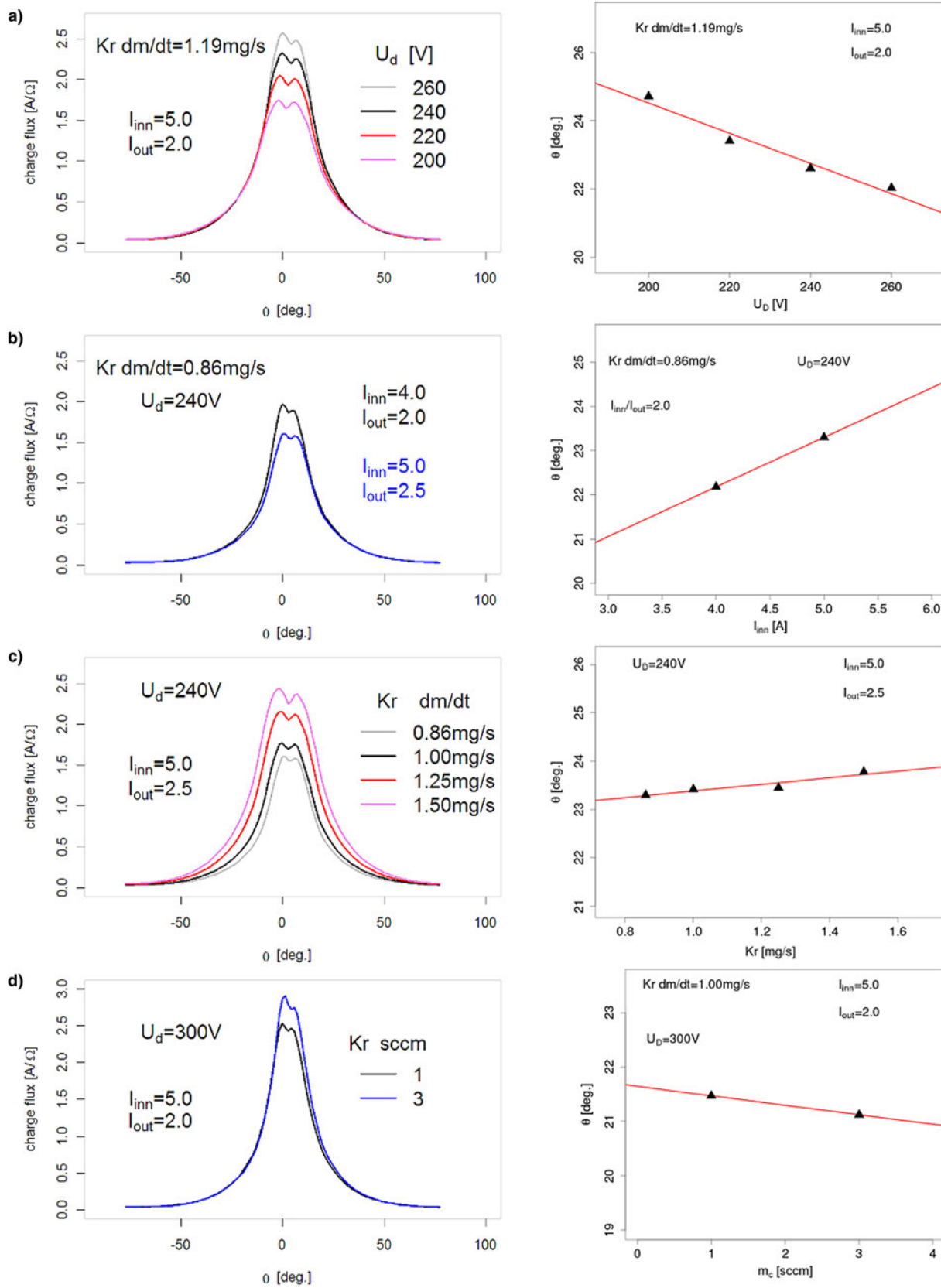


Fig. 4. The 2D profiles and divergence angles with respect to (a) discharge voltage, (b) coil currents, (c) anode mass flow rate, and (d) cathode mass flow rate.

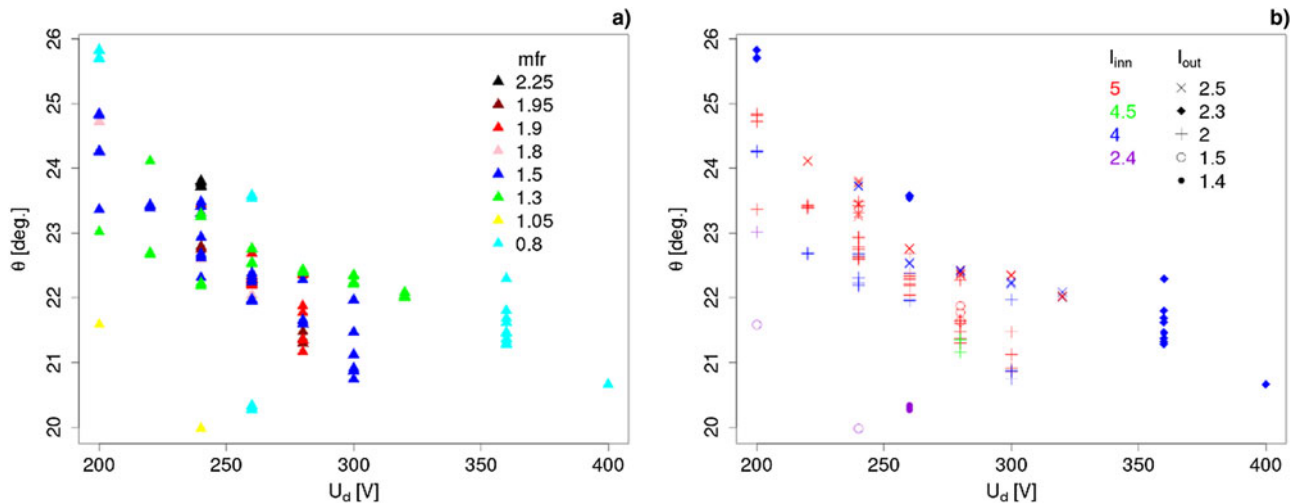


Fig. 5. Divergence angles for all investigated cases with respect to discharge voltage. Legends correspond to (a) mass flow rate and (b) coil currents.

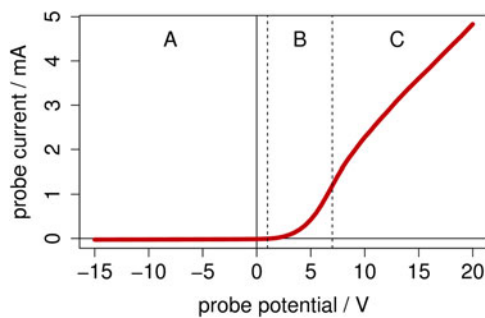


Fig. 6. Example of Langmuir probe current-voltage characteristic for a cylindrical probe. (a) Ion saturation current, (b) transition region, (c) electron saturation current.

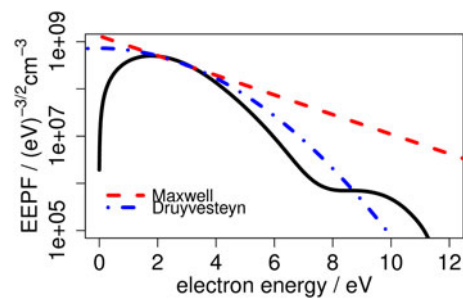


Fig. 8. Electron energy probability function with fitted Maxwell and Druyvesteyn distributions.



Fig. 7. Langmuir probe manufactured in the PlANS laboratory.

of KLIMT (discharge voltage 200–300 V, mass flow rate 1.00, 1.25 mg/s) for both gases (krypton and xenon) are shown in Figure 9. The magnetic field inside the discharge channel was adjusted with different values of coil currents to provide the most stable operation of the thruster, but was fixed throughout individual data series to allow for easier interpretation of the results.

Obtained values of plasma parameters are comparable with plasma characteristics that were reported for thrusters of similar design (Dannenmayer *et al.*, 2009; Lobbia and Gallimore, 2010). Plasma space potential, electron temperature, and electron concentration all seem to rise with the discharge voltage. Higher electron temperatures for bigger voltages may be due to higher kinetic energies of the expelled ions, which grab the electrons from the cathode. Also, it was noted that for the same discharge voltages, krypton exhibits lower electron temperatures than xenon. The reason for this is not yet clear, but is believed to stem from the fact that xenon is over 1.5 times more massive, so the energy transfer between electrons and xenon ions is less effective than for krypton and the electrons cool slower. For the same reason, electron concentration is higher for krypton – for the same mass flow rate, there are much more krypton ions than xenon ions in the plasma. An increase in the electron concentration that was observed for increasing discharge voltage is consistent with the Faraday probe results in which the beam divergence is lower for higher voltages (Fig. 4). Moreover, for higher mass flow rates, the beam divergence increases so the net result on electron concentration may be either positive or negative, what was also observed.

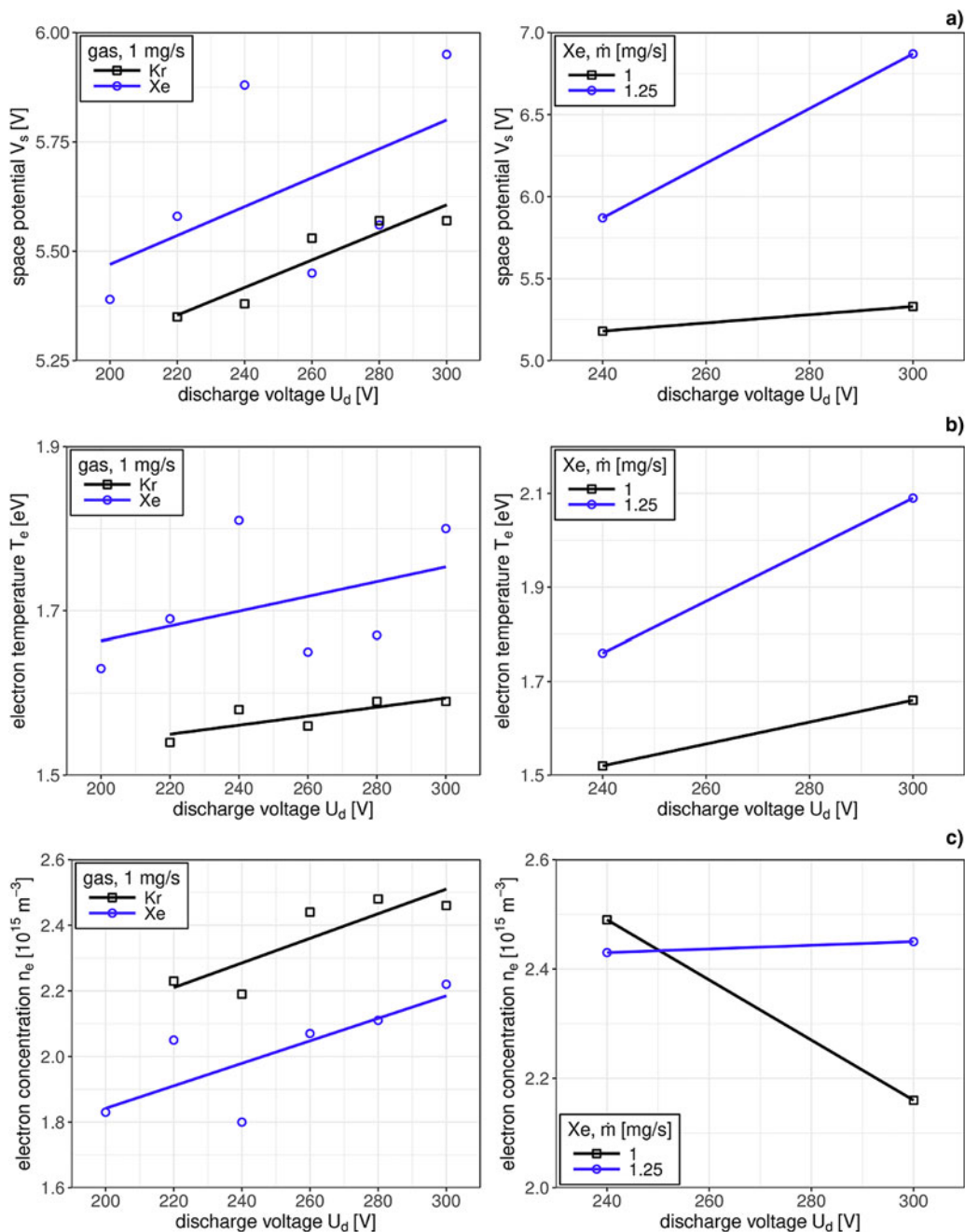


Fig. 9. (a) Space potential V_s , (b) electron temperature T_e , and (c) electron concentration n_e as a function of discharge voltage U_d for different working conditions of KLIMT.

Conclusions

All the obtained results, both from Faraday and Langmuir probes, seem to be consistent with our understanding of the Hall thruster plasma beam formation. In particular, it was observed that increasing of the discharge voltage results in less divergent beam and so higher electron concentration in the thruster axis. Additionally, higher ion energies obtained in this way produce higher plasma potentials and electron temperatures. Moreover, bigger mass flow rates do not result in much larger electron concentration because at the same time the beam divergence also grows.

Next step in the design of beam diagnostics for the PlaNS laboratory will be to prepare our own Faraday probe and produce a movable arm to allow for spatial measurements of the charge flux and plasma parameters. Additionally, an enhanced acquisition system for Langmuir probe will be manufactured to compensate stray effects not addressed in the first version (e.g., addition of chamber wall sheath in the probe circuit resistance) and make acquisition process more automatic to allow for higher number of data points to be taken.

Acknowledgments. Above results were presented on the Plasma 2017 conference in Warsaw organized by the Institute of Plasma Physics and Laser

Microfusion. The studied 0.5 kW Hall thruster was developed in the scope of ESA/PECS Contract No. 4000107746/13/NL/KLM – Krypton Large Impulse Thruster. Authors would like to thank Ms Kathe Dannenmayer, head of ESA Electric Propulsion laboratory in which part of the measurements was conducted, for her support.

References

- Boeuf JP** (2017) Tutorial: physics and modeling of Hall thrusters. *Journal of Applied Physics* **121**, 011101.
- Brown DL** (2009) *Investigation of Low Discharge Voltage Hall Thruster Characteristics and Evaluation of Loss Mechanisms*. (PhD Thesis). University of Michigan.
- Chen FF** (2003) Lecture notes on Langmuir probe diagnostics, mini-course on plasma diagnostics. *IEEE-ICOPS Meeting*.
- Chen FF, Evans JD and Arnush D** (2002) A floating potential method for measuring ion density. *Physics of Plasmas* **9**, 1449.
- Conde L** (2011) An introduction to Langmuir probe diagnostics of plasmas. Available online at <http://plasmalab.aero.upm.es/~lcl/PlasmaProbes/Probes-2010-2.pdf> (accessed 18 June 2018).
- Dannenmayer K, Kudrna P, Tichy M and Mazzoufre S** (2009) Time-resolved measurement of plasma parameters in the far-field plume of a low-power Hall effect thruster. *Plasma Sources Science and Technology* **21**, 055020.
- Druyvesteyn MJ** (1930) Der Niedervoltbogen. *Zeitschrift für Physik* **64**, 781.
- Godyak VA and Alexandrovich BM** (2015) Comparative analyses of plasma probe diagnostics techniques. *Journal of Applied Physics* **118**, 233302.
- Godyak VA and Demidov VI** (2011) Probe measurements of electron-energy distributions in plasmas: what can we measure and how can we achieve reliable results? *Journal of Physics D: Applied Physics* **44**, 233001.
- Goebel DM and Katz I** (2008) *Fundamentals of Electric Propulsion: Ion and Hall Thrusters*. New Jersey: John Wiley & Sons.
- Kurzyna J, Barral S, Daniilko D, Miedzic J, Bulit A and Dannenmayer K** (2014) First tests of the KLIMT Thruster with Xenon propellant at the ESA propulsion laboratory. *Space Propulsion 2014 Proceeding*.
- Kurzyna J, Szelecka A, Daniilko D, Barral S, Dannenmayer K, Bosch Borras E and Schönherr T** (2016) Testing KLIMT prototypes at IPPLM and ESA propulsion laboratories. *Space Propulsion 2016 Proceeding*.
- Lobbia RB and Gallimore AD** (2010) Temporal limits of a rapidly swept Langmuir probe. *Physics of Plasmas* **17**, 073502.
- Merlino RL** (2007) Understanding Langmuir probe current-voltage characteristics. *American Journal of Physics* **75**, 12.
- Morozov AI** (2003) The conceptual development of stationary plasma thrusters. *Plasma Physics Reports* **29**, 235.
- Raites Y, Staack D, Smirnov A and Fisch NJ** (2005) Space charge saturated sheath regime and electron temperature saturation in Hall thrusters. *Physics of Plasmas* **12**, 073507.
- Steinbruchel C** (1990) A new method for analyzing Langmuir probe data and the determination of ion densities and etch yields in an etching plasma. *Journal of Vacuum Science & Technology A* **8**, 1663.
- Szelecka A, Kurzyna J and Bourdain L** (2017) Thermal stability of the krypton Hall effect thruster. *NUKLEONIKA* **62**, 9–15.
- Zhurin VV, Kaufman HR and Robinson RS** (1999) Physics of closed drift thrusters. *Plasma Sources Science and Technology* **8**, R1–R20.